the bottom, there are a p-InP substrate (3·0 μm), a p-InP cladding layer (0·5 μm), a p-InGaAsP active layer (0·1 μm), an n-InP cladding layer ((a) 0·11 μm, (b) 0·10 μm), and an n-Inp top layer (3·0 μm). The current blocking layers of Fig. 2*a* are n-InP (1×10^{18} cm^{-3}, 0·2 μm), p-InP (1×10^{18} cm^{-3}, 0·5 μm), and p-$In_{0.46}Al_{0.54}As$ (1×10^{18} cm^{-3}, 100 Å; 0·4% strain). In Fig. 2*b* there are no InAlAs layers.

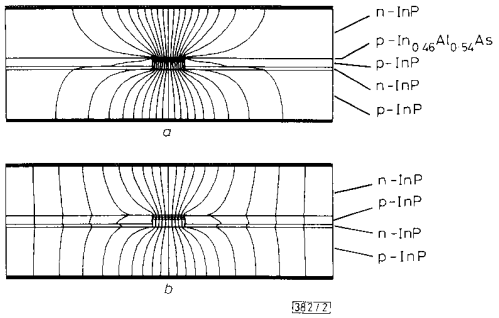

Fig. 2 *Calculated current-flow distributions at 85°C in planar BH lasers*

a *pnpn* blocking layers including 100 Å strained $In_{0.46}Al_{0.54}As$ layer

b Conventional blocking layers

The thickness of p- and n-InP blocking layers are 0·5 μm and 0·2 μm, respectively

The current-flow distributions at 85°C in Fig. 2 are at an optical power of 2–3 mW. It is found that, by employing the widegap InAlAs layers, the leakage current is suppressed in spite of the thin blocking structure (~0·7 μm). This is because the widegap InAlAs suppresses the electron injection from the n-InP top layer to the n-InP floating layers.

Fig. 3 shows light output-current (L/I) characteristics of planar BH lasers at 85°C, which were also obtained using the two-dimensional simulation. The L/I curves are shown for different AlAs mole fractions in InAlAs blocking layers, as shown in Fig. 2*a*. Using the $In_{1-x}Al_xAs$ with $x \geq 0{\cdot}54$, we can avoid the leakage current, thereby significantly improving the differential quantum efficiency and threshold current up to 85°C. As the tensile strain is only 0·4% in $In_{0.46}Al_{0.54}As$, the assumed thickness (100 Å) is much smaller than the critical thickness of Matthews and Blakeslee.[8] Moreover, the tunnel current is negligible for this thickness. In addition, it is easy to fabricate BH lasers or buried crescent layers[9] with *pnpn* structures including the widegap layers, because of the 'flatness' of these layers. Finally, it should be noted that, for widegap blocking layers, we can use not only III-V group compounds but also II-VI compounds, whose lattice constants are similar to InP.

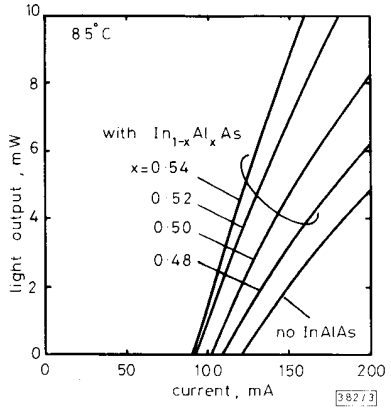

Fig. 3 *Calculated light output-current characteristics of planar BH lasers with different AlAs mole fractions in InAlAs blocking layers at 85°C*

InAlAs layer thickness is 100 Å

In conclusion, we have shown theoretically that the leakage current in BH lasers at high temperature can be drastically reduced by employing widegap InAlAs strained layers.

Acknowledgment: The authors wish to thank Dr. K. Yamaguchi for his useful discussion.

T. OHTOSHI
N. CHINONE

Central Research Laboratory
Hitachi Ltd.
Kokubunji, Tokyo 185, Japan

15th October 1990

References

1 OHTOSHI, T., YAMAGUCHI, K., and CHINONE, N.: 'Analysis of current leakage in InGaAsP/InP buried heterostructure lasers', *IEEE J*, 1989, **QE-25**, pp. 1369–1375

2 ASADA, S., SUGOU, S., KASAHARA, K., and KUMASHIRO, S.: 'Analysis of leakage current in buried heterostructure lasers with semi-insulating blocking layers', *IEEE J*, 1989, **QE-25**, pp. 1362–1368

3 ASAI, H., and OE, K.: 'Energy band-gap shift with elastic strain in $Ga_xIn_{1-x}P$ epitaxial layers on (001) GaAs substrates', *J. Appl. Phys.*, 1983, **54**, pp. 2052–2056

4 ADACHI, S.: 'Material parameters of $In_{1-x}Ga_xAs_yP_{1-y}$ and related binaries', *J. Appl. Phys.*, 1982, **53**, pp. 8775–8792

5 ADACHI, S.: 'GaAs, AlAs, and $Al_xGa_{1-x}As$: Material parameters for use in research and device applications', *J. Appl. Phys.*, 1985, **58**, pp. R1–R29

6 CASEY, H. C., JUN., and PANISH, M. B.: 'Heterostructure lasers Part B' (Academic Press, New York, 1978)

7 OHTOSHI, T., YAMAGUCHI, K., NAGAOKA, C., UDA, T., MURAYAMA, Y., and CHINONE, N.: 'A two-dimensional device simulator of semiconductor lasers', *Solid-State Electron.*, 1987, **30**, pp. 627–638

8 MATTHEWS, J. W., and BLAKESLEE, A. E.: 'Defects in epitaxial multilayers, I: Misfit dislocations', *J. Cryst. Growth*, 1974, **27**, pp. 118–125

9 OOMURA, E., HIGUCHI, H., SAKAKIBARA, Y., HIRANO, R., NAMIZAKI, H., SUSAKI, W., IKEDA, K., and FUJIKAWA, K.: 'InGaAsP/InP buried crescent laser diode emitting at 1·3 μm wavelength', *IEEE J.*, 1984, **QE-20**, pp. 866–874

HIGH POWER SWITCHING OF MULTIELECTRODE BROAD AREA LASERS

Indexing terms: Lasers, Semiconductor lasers

24 ps optical pulses of peak power in excess of 1·3 watts are continuously generated at GHz repetition rates using a GaAs/AlGaAs single quantum well broad area laser with an intracavity loss modulator. Efficient high power light modulation is also demonstrated with the same structure.

There is some interest in generating continuous, high peak power (watts), picosecond optical pulses at GHz repetition rates e.g. to deliver data or clock pulses to self electro-optic effect devices (SEEDs). Such power and speed requirements are a challenge to conventional laser designs. Direct gain modulation of single stripe semiconductor lasers is a well known and convenient method of generating controlled picosecond optical pulses[1–3] without the strictures imposed by mode locking. Although gain switched optical pulses of less than 4 ps duration have been generated at a repetition rate of 100 MHz with a narrow single stripe MQW laser,[2] this method of optical pulse generation, together with mode locking, has only occasionally been applied to high power laser structures.[4,5] Van der Ziel *et al.*[4] demonstrated 62 ps optical pulses at a 960 MHz repetition rate with a gain switched MQW phased array, and recently Masuda *et al.*[5] have generated 26 ps optical pulses from a mode locked external cavity quantum well phased array.

A difficulty in achieving high power, ultrashort optical pulses with gain switched broad area lasers, is the large peak current (tens of amps) which must be delivered to the laser

active region over a short time scale ($\ll 1$ ns). We have circumvented this requirement by modulating the absorption of a small section of a segmented broad area laser. This scheme relaxes drive current requirements as the carrier density required for lasing is no longer supplied by the switching electrical signal but by a fixed DC gain section current I_G. We report generation of 24 ps optical pulses of peak power in excess of 1·3 W at GHz repetition rates by absorption modulation of a GaAs/AlGaAs broad area single quantum well laser. These results are achieved by application of a modest 4 V modulation to a 50 Ω terminated intracavity absorber. In addition we use the structure to achieve efficient high power digital optical modulation.

After crystal growth,* broad area single quantum well lasers of length $L_C = 500\,\mu$m and of stripe width $40\,\mu$m with an intracavity loss modulator were created by application of three photolithographically-defined metal contacts to the top layer. The area intervening the metal contacts was etched $0{\cdot}3\,\mu$m down to increase the isolation resistance between the contacts. The resulting structure is shown in the inset of Fig. 1. Also shown in Fig. 1 are the pulsed light-current curves of these devices for a number of applied absorber voltages V_S. Efficient voltage modulation of the laser threshold is observed. We have generated ultrashort optical pulses by DC biasing the gain section of the device and applying an electrical impulse train (derived by amplification of the differentiated output of a pattern generator) to the absorber section which is correctly terminated by a 50 Ω chip resistor. The peak voltage applied is 4 V in a pulse of 110 ps full width half maximum (FWHM).

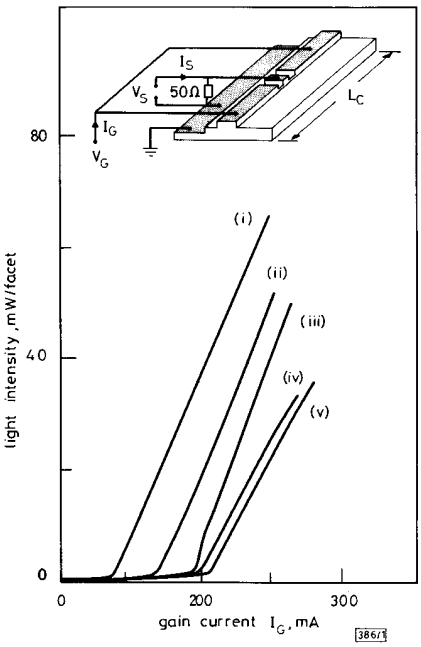

Fig. 1 *Pulsed light-current characteristics of segmented broad area laser for a number of applied absorber voltages V_S*

(i) $V_S = 2{\cdot}0$ V (ii) $V_S = 1{\cdot}0$ V (iii) $V_S = 0$ V (iv) $V_S = -1{\cdot}0$ V (v) $V_S = -2{\cdot}0$ V

Inset: schematic diagram of the broad area structure used

In Fig. 2 we show the measured optical output when a continuous electrical impulse train at 1·49 GHz is applied to the absorber section and the constant gain section current is $I_G = 350$ mA. Fig. 2*a* shows a portion of the optical pulse train illustrating the high contrast ratio of the optical pulses and, importantly, the absence of satellite or subpulses accompanying the main pulse. In Fig. 2*b* we show a detail of a single pulse from the train. Deconvolving the detected 37 ps pulse width (FWHM) from the measured sampling oscilloscope/photodiode impulse response time (FWHM, 28 ps), the optical pulse width is 24 ps FWHM. This, to our knowledge, is the shortest duration optical pulse generated with broad area or phased array lasers by either gain switching or mode locking. The average power output per facet was 48 mW yielding, for the pulses of Fig. 2, a peak power in excess of 1·3 W per facet.

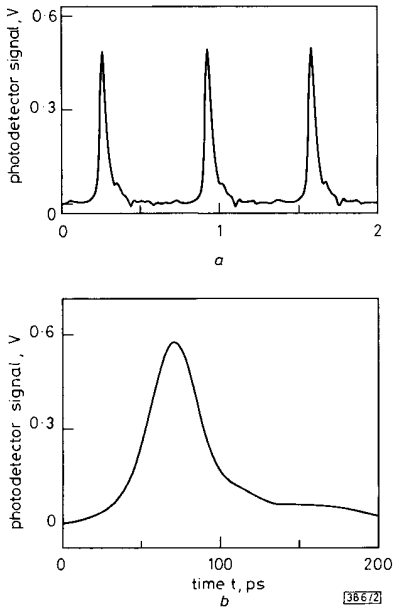

Fig. 2 *Measured optical output when 1·496 Hz continuous electrical impulse train is applied to absorber segment*

Absorber segment biased at −0·8 V
Gain section current is $I_C = 350$ mA
Electrical pulse of width 110 ps FWHM and 4 V peak at 1·49 GHz
a detected optical output
b detail of single pulse

In Fig. 3 we show the optical output when the gain section is biased at $I_G = 195$ mA and a non-return to zero $-0{\cdot}5 < V_S < 2{\cdot}5$ V pseudorandom digital data stream at 700 Mbit/s is applied to the absorber section. Although sub-

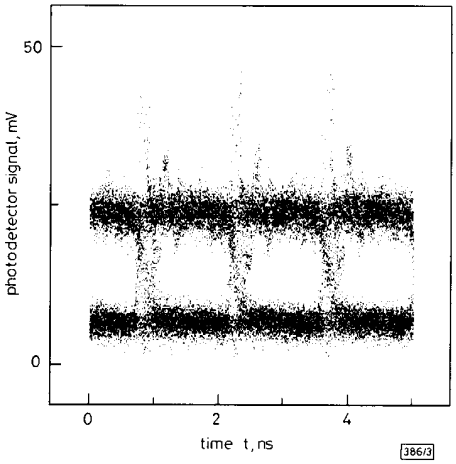

Fig. 3 *Received eye pattern when $-0{\cdot}5 < V_S < 2{\cdot}5$ V pseudo random bit stream at 700 Mbit/s is applied to absorber section S*

$I_G = 195$ mA

* HOBSON, W. S., LEVI, A. F. J., O'GORMAN, J., PEARTON, S. J., ABERNATHY, C. R., and SWAMINTHAN, V.: 'GRINSCH GaAs/AlGaAs laser structures grown by OMVPE using a novel aluminum source' (unpublished)

stantial optical power is switched (≈50 mW/facet) a purely digital response is compromised by substantial ringing which accompanies the switching transient giving rise to the shape of the eye pattern.

Broad area lasers exhibit an enhanced relaxation oscillation in their transient operation, due possibly to mode coupling effects between different transverse modes of the structure. Similar behaviour has been seen in phased array structures.[6] These pronounced oscillations are responsible for the appearance of the eye pattern of Fig. 3 and are also to a certain extent responsible for the brevity of the optical pulses which we have reported. The shortest pulses result when a resonance exists between the impulse train and the laser transient response, otherwise the shortest optical pulse width was about 30 ps (FWHM). It should also be noted that the lasers used in this work were as cleaved. As the laser facets are uncoated, significantly larger output powers would be attained by optimising the power extracted from the cavity by application of high and low reflectivity coatings to the facets (leaving the laser threshold substantially unchanged). A shorter laser cavity may further reduce the optical pulse duration.

In conclusion, we have used a simple modification of a broad area laser to generate shorter optical pulses with greater peak power than previously reported for gain switched or mode locked broad area or phased array lasers. This has been achieved by application of modest electrical impulses to an intracavity loss modulator. We finally note that our results have considerable implications for ultrashort pulse generation with high power lasers. Broad area lasers offer significant fabrication advantages in comparison to more advanced structures such as phased arrays. As large and rapid gain (or loss) modulation is required for subpicosecond pulse generation by active mode locking of semiconductor lasers,[8] it is apparent that shorter pulse durations than heretofore obtained will be achieved by use of monolithic loss modulators in actively mode locked external cavity broad area lasers. Furthermore, it has recently been shown that by growth on appropriately oriented substrates, filamentation in broad area lasers can be prevented.[9] Consequently the external cavity can then be effectively used as a modal filter to force high power, mode locked operation in the fundamental transverse mode.

J. O'GORMAN
A. F. J. LEVI
W. S. HOBSON

AT&T Bell Laboratories
Murray Hill, New Jersey 07974, USA

16th October 1990

References

1 ITO, H., YOKOYAMA, H., MURATA, S., and INABA, H.: 'Picosecond optical pulse generation from an RF modulated AlGaAs D.H. diode laser', *Electron. Lett.*, 1979, **15**, (23), pp. 738–740

2 BIMBERG, D., KETTERER, K., BÖTTCHER, E. H., and SCHOLL, E.: 'Gain modulation of unbiased semiconductor lasers: ultrashort light-pulse generation in the 0·8 μm to 1·3 μm wavelength range', *Int. J. Electron.*, 1986, **60**, pp. 23–45

3 NAGARAJAN, R., KAMIYA, T., KASUKAWA, A., and OKAMOTO, H.: 'Observation of short (<4 ps) gain-switched optical pulses from long-wavelength multiple quantum well lasers', *Appl. Phys. Lett.*, 1989, **55**, pp. 1273–1275

4 VAN DER ZIEL, J. P., TEMKIN, H., LOGAN, R. A., and DUPUIS, R. D.: 'High power picosecond pulse generation in GaAs multiquantum well lasers arrays using pulsed current injection', *IEEE J. Quantum Electron.*, 1984, **QE-20**, pp. 1236–1242

5 MASUDA, H., and TAKADA, A.: 'Picosecond optical pulse generation from mode-locked laser diode array', *Electron. Lett.*, 1989, **25**, (21), pp. 1418–1419

6 ELLIOTT, R. A., DE FREEZ, R. K., PAOLI, T. L., BURNHAM, R. D., and STREIFER, W.: 'Dynamic characteristics of phase-locked multiple quantum well injection lasers', *IEEE J. Quantum Electron.*, 1985, **QE-21**, pp. 598–602

7 ASPIN, G. J., CARROLL, J. E., and PLUMB, R. G.: 'The effect of cavity length on picosecond pulse generation with highly rf modulated AlGaAs double heterostructure lasers', *Appl. Phys. Lett.*, 1981, **39**, pp. 860–861

8 BOWERS, J. E., MORTON, P. A., MAR, A., and CORZINE, S. W.: 'Actively mode-locked semiconductor lasers', *IEEE J. Quantum Electron.*, 1989, **QE-25**, pp. 1426–1439

9 CHANG-HASNAIN, C. J., KAPON, E., and BHAT, R.: 'Spatial mode structure of broad-area semiconductor quantum well lasers', *Appl. Phys. Lett.*, 1989, **54**, pp. 205–207

ARQ SCHEME WITH COMBINED CHANNEL CODING AND MODULATION USING NONCOHERENT DETECTION

Indexing terms: Modulation, Detection

A new method for the combination of channel coding and modulation with noncoherent detection in automatic-repeat-request protocols is described. This scheme can be used in automatic-repeat-request protocols in which each codeword is transmitted $m \geq 2$ times consecutively. Theoretical analysis shows that this scheme offers a net increase in the performance with respect to other similar protocols.

Automatic-repeat-request (ARQ) protocols are often used to improve the reliability of communication systems on many real channels. However, ARQ schemes often present low information throughput, because they must retransmit the messages detected in error. In some ARQ protocols the same message is transmitted m times consecutively to improve the throughput.[1,2] Recently, a new scheme, which combines the modulation and channel coding in ARQ protocol has been introduced.[3] This scheme, denoted in the following as MARQ, permits a significant enhancement in throughput of an ARQ protocol.

The performance of the MARQ scheme depends on the Euclidean distances among modulated signals. In the MARQ scheme these distances increase linearly with the number of transmissions of a message. However, ARQ protocols with $m \geq 1$ transmission per codeword, in which the Euclidean distances increase more quickly than linearly, have been proposed.[3,4] These methods require a coherent detection of the received signal.

In this letter a new method, denoted as MARQ1, for the combination of modulation and channel coding in an ARQ protocol using noncoherent detection is presented. The ARQ scheme transmits m copies each time a message must be sent. Binary continuous-phase frequency shift modulation (CPFSK) is assumed, but the procedure can be easily extended to other modulation schemes.

Let us consider the ARQ protocols in which a message detected in error is retransmitted m times consecutively.[4] In these protocols m equal copies of the same message are transmitted. The combination of the modulation in the coding operation through the ARQ scheme with memory described by Benelli[4] permits a linear improvement in the Euclidean distances.

In the scheme considered here each block of k information symbols is encoded in a codeword $c = \{c_i\}$ through a code C, n symbols long. In the classical schemes each symbol c_i, before its transmission, is sent to a CPFSK modulator, which associates to it a waveform $s_i(t)$, T seconds long. Let us consider a transmission cycle of c. In our scheme the transmitter associates to c_i a waveform $s_i(t)$, mT seconds long, given by

$$s_i(t) = (\sqrt{2E/T}) \cos [2\pi f_0 t + (\pi h t/T)c_i + x_i] \quad (1)$$

for $[(i-1)m+1]T \leq t \leq imT$, f_0 being the carrier frequency, h the modulation index and x_i a phase term. Therefore, a signal vector $s(t) = \{s_i(t)\}$, mT seconds long, is associated to the codeword c.

Each time a transmission of c is received, the receiver evaluates the two distances $d_i^2(1)$ and $d_i^2(-1)$ between the received signal in the ith interval ($1 \leq i \leq n$) and the waveform $s_i(t)$ associated to the symbol $+1$ and -1, respectively. For each symbol, the receiver forms a distance cumulative report $D_i(j)$ defined as

$$D_i(j) = D_i(j-1) + d_i^2(1) - d_i^2(-1) \quad (2)$$

being $D_i(0) = 0$. When the distances $D_i(j)$ have been updated for all the n bits, the demodulator performs a hard detection of each component. A binary vector $w = (w_1, w_2, \ldots, w_n)$ is constructed, having the ith component defined as

$$w_i = \text{sign } D_i(j) \quad (3)$$